

# A high speed noncommunication protection scheme for power transmission lines based on wavelet transform

Ammar A. Hajjar

Electrical Power Department, Faculty of Mechanical and Electrical Engineering, Tishreen University, Latakia, Syria

## ARTICLE INFO

### Article history:

Received 30 January 2012

Received in revised form 5 October 2012

Accepted 30 October 2012

Available online 23 December 2012

### Keywords:

Wavelet transform

High-speed protection

Noncommunication scheme

Transmission lines

Transient currents

## ABSTRACT

This paper presents a high-speed protection scheme for power transmission lines based on wavelet transform (WT). It is a noncommunication protection scheme as it depends completely on locally measured currents. It utilizes WT, which acts as a multi-level bandpass filter, to extract two distinct bands of frequency from the fault induced high frequency (HF) transient currents; the first band is high while the second band is relatively lower. The spectral energies of the extracted signals are then calculated to form two discriminating signals of the relay (operative and restraint). Based on the ratio between these discriminating signals the relay can distinguish whether a fault is internal or external to the protected line.

The performance of the introduced protection scheme was evaluated by simulating several faults on 400 kV–50 Hz transmission system using an electro magnetic transient program (EMTDC). The simulation results showed distinct performance of the scheme irrespective of the fault type, fault inception angle, fault position and fault resistance. Moreover, it is not affected by a system configuration and system source parameters.

© 2012 Elsevier B.V. All rights reserved.

## 1. Introduction

EHV transmission lines protection schemes can be classified into two main categories: the communication and noncommunication protection schemes. However, each of the aforesaid protection schemes has its own problems. In this respect, the problems of the noncommunication protection schemes, such as distance protection, are: it cannot protect the entire line and its setting is not easy. In this context, the communication protection schemes, such as differential protection, were solved the aforesaid problems, but they need an expensive and complicated communication system. Furthermore, the reliability and cost of the communication protection schemes are function of the reliability and cost of the used communication systems [1]. Hence, a high-speed, low cost and reliable noncommunication protection scheme for the entire transmission line protection is required.

In this respect, the communication protection schemes [2,3] and noncommunication protection schemes [4,5] based on transient components were offered a high-speed protection of the entire line. However, they suffered from several limitations, such as not being able to detect faults with zero phase inception angles, high resistance faults and are affected by any change in a system configuration and system source parameters.

To get rid of the aforesaid limitations, the authors of [6,7] presented a noncommunication protection scheme based on capturing the fault generated HF transient voltages with the help of line traps and stack tuners. They designed special bandpass filters, with 17 floating point coefficients, to extract two distinct signals from the captured signals in order to form the operative and restraint signals and hence to distinguish whether the fault is internal or external to the protected line. However, installing line traps and stack tuners at each end of the line increases the cost and limits the application of the scheme. To solve the aforesaid problem the author of [8] presented an alternative form of noncommunication protection scheme based on the fault generated HF transient currents that does not require line traps and stack tuners. However, the technique in [8] alone has difficulty in distinguishing between a fault on the line close to remote busbar within the protected zone and on the busbar or close to the busbar outside the protected zone. In addition, the use of two needless modal signals in [8] to cover all types of faults at low speed specially designed multi channels filter, with 8 floating point coefficients, may limit its application. The authors of [9] used the so-called 'Chaari' recursive complex WT [10] to extract the aforesaid two distinct bands of frequency. However, the recursive WT requires historical and future data and requires a large number of computations; e.g., it needs 36 real multiplications and 35 real additions for each sample [10]. The authors of [11] used the 'db4' wavelet, which has a bandpass filter of 8 floating-point coefficients, to extract the abovementioned bands of frequency. The authors of [12] augmented the scheme of [8] with line traps

E-mail addresses: [ammahajjar@hotmail.com](mailto:ammahajjar@hotmail.com), [ammahajjar@tishreen.edu.sy](mailto:ammahajjar@tishreen.edu.sy)

and used an improved recursive WT that depends only on a historical data. Moreover, they used phase information to discriminate the faulted line. However, in addition to a large number of computations required by the scheme, installing line traps increases the scheme cost and limits its application.

It is obvious from the above survey that the filtering algorithm is the core of the non-communication protection scheme. Hence, suitable choice of the filtering algorithm, in terms of speed and time frequency localization, plays a vital role. Therefore, this paper uses a high-speed wavelet “Piecewise Linear Spline Wavelet”, which has a bandpass filter with 3 coefficients, for developing a high-speed noncommunication protection scheme for EHV transmission lines. In this respect, the WT was used to capture two bands of frequencies from the fault induced HF transient currents. The spectral energies of these bands were used for faulted line discrimination. Computer simulation of the scheme showed that the scheme has a high-speed response and distinct performance irrespective of the fault type, fault inception angle, fault position and fault resistance.

### 2. Theory of wavelet transform

Wavelet is a waveform of effectively limited duration that has an average value of zero. WT is relatively a new signal processing tool for transient signals analysis. It breaks up a signal into shifted and scaled (compressed or dilated) versions of the mother wavelet (basis function). WT has some unique features that make it more suitable for transient signals analysis in a power system [9–13], such as:

- It has the property of time-frequency localization, even, of a small disturbance in a signal.
- WT has a strong capability of extracting the signal components under different frequency bands while retaining the time domain information.

The continuous WT (CWT) of a time dependent signal  $f(t)$ , is defined as the sum over all times of a signal  $f(t)$  multiplied by a scaled and shifted versions of a mother wavelet  $\psi(t)$ . The mother wavelet  $\psi(t)$  can be defined as follows:

$$\psi_{b,a}(t) = \frac{1}{\sqrt{a}} \psi\left(\frac{t-b}{a}\right) \tag{1}$$

where “ $a$ ” and “ $b$ ” represent the time scaling and shifting, respectively. The coefficients  $C_f(a, b)$ , or the CWT, are defined by the following inner product:

$$C_f(a, b) = \int_{-\infty}^{+\infty} f(t) \cdot \psi_{b,a}^*(t) \cdot dt \tag{2}$$

where “\*” refers to a complex conjugate.

WT of a sampled signal can be obtained using the discrete WT (DWT) relation:

$$DWT(m, n) = \frac{1}{\sqrt{a_0^m}} \sum_k f(k) \psi^*\left(\frac{n - ka_0^m}{a_0^m}\right) \tag{3}$$

where the parameters  $a$  and  $b$  in (1) are replaced by  $a_0^m, ka_0^m$ , respectively,  $n, k, a_0$  are integers;  $a_0$  is some selected spacing factor (usually chosen equal to “2” for dyadic grid), and  $m$  is the scaling index 0, 1, 2, 3, ...

Generally, WT consists of successive pairs of low and high pass filters [14,15]. For each pair the high-scale, low frequency components of the signal  $f(t)$  are called approximations (CA), while the low-scale, high frequency components of the same signal  $f(t)$  are called details (CD). After each filtering stage, every second data point is thrown away to avoid redundant data. Fig. 1 depicts the two stages filtering process of a signal  $f(t)$ .

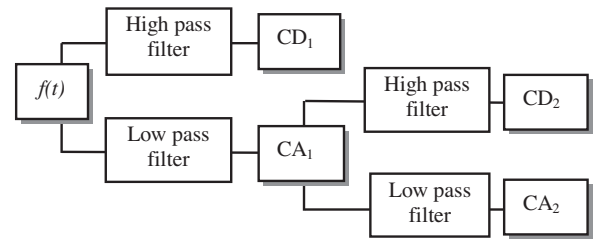


Fig. 1. Two stages filtering process of a signal  $f(t)$ .

### 3. Principle of the noncommunication protection

If a fault occurs on a transmission line a wideband of HF transient current signals will be induced at the fault point, then they will travel toward the line’s busbars, which constitute a discontinuity points. Accordingly, part of the signals will continue along the adjacent line(s) while the rest will reflect back and forth between a fault point and the line’s busbars until a post fault steady state is reached.

The principle of a noncommunication protection scheme can be explained using a 400kV transmission system (shown in Fig. 2); the lengths of lines are given in figure. The protection relay ‘ $R_{yz}$ ’ is assumed to be installed on line ‘ $L_2$ ’ near busbar ‘ $Y$ ’, and is responsible for the protection of the entire line ‘ $L_2$ ’.  $C_s$  represents the stray capacitance of the busbar (typically 0.1  $\mu$ F [6–10]) that has low impedance at high frequency and high impedance at low frequency. In this context, a busbar is normally connected to many power equipments such as power transformers and generating units, the characteristics of these equipments will determine the busbar to ground impedance that is normally conductive in nature. However, at significant high frequencies, the capacitance and capacitive coupling become the dominant factor in the busbar impedance [6,8]. Therefore, a significant amount of the transient current, particularly the higher frequency components, will be shunted to ground through the busbar capacitance. This feature is the key to develop a noncommunication protection scheme in which the busbars at both ends of a protected line can be used as boundaries to the protected zone [8]. When an external fault occurs on a transmission system shown in Fig. 2, e.g., at point  $F_2$  on line ‘ $L_3$ ’, the transient current signal  $I_2$ , which contains wideband of HF components, will travel toward busbar ‘ $Z$ ’. When this signal reach busbar ‘ $Z$ ’ part of it,  $I_1$ , will continue to travel into line ‘ $L_2$ ’, and the rest,  $I_0$ , will be shunted into ground by a busbar capacitance. As a result, the relay ‘ $R_{yz}$ ’ will measure an attenuated current,  $I_1$ , rather than the initial current  $I_2$ . However, the attenuation will be larger at higher frequency than that at lower frequency since the busbar impedance into ground decreases with increasing frequency. In contrast, there is no such attenuation in case of an internal fault, e.g., a fault at point  $F_1$  on line  $L_2$ . This important feature can be used to discriminate between internal and external faults.

The introduced high-speed noncommunication protection scheme depends on using high-speed WT, which acts as a multi-level bandpass filter, to capture two distinct bands of frequency, one of low frequency level and the other of higher frequency level. The ratio of the spectral energies of the higher band to the lower band will be used to discriminate between external and internal faults.

### 4. Relay design description

A block diagram of the introduced protection scheme is shown in Fig. 3.

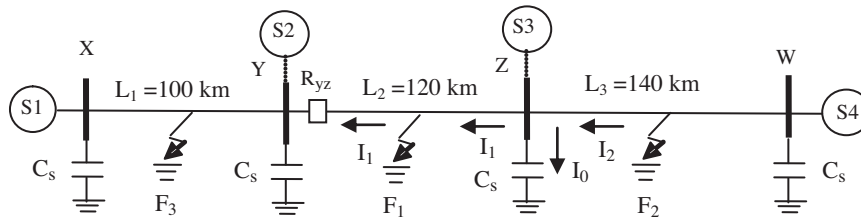


Fig. 2. A one line diagram of the studied transmission system.

4.1. Modal current signal

To eliminate any noise induced in the line due to mutual coupling between adjacent parallel lines and/or multiple circuits sharing the same right of way, the outputs of the CT's ( $I_a$ ,  $I_b$  and  $I_c$ ) are combined in order to form a modal current signal as follows:

$$I_m = I_a - 2I_b + 2I_c \tag{4}$$

This modal signal is sufficient to cover all types of faults that encountered in practice; and ensures immunity to all disturbances other than those associated with the protected line. It is worth mentioning that the introduced scheme can be applied directly to phase

currents ( $I_a$ ,  $I_b$  and  $I_c$ ), but in so doing the computation burden will be increased (three phase signals will be processed instead of one modal signal). Moreover, the relay stability will be jeopardized under external faults due to a mutual coupling.

4.2. Anti aliasing filter

To avoid any error in a subsequent digital signal processing arising due to signal aliasing (arising false frequencies in a signal) the modal signal is passed through an analog 2nd order Butterworth filter with a cutoff frequency of around half the digital sampling frequency. In so doing, any unwanted high frequencies (noise) can be removed before sampling.

4.3. A high-speed wavelet for noncommunication protection

Digital decomposition filter constitute the main part of a non-communication protection relay. Therefore, suitable choice of this filter, in terms of speed and time-frequency localization, plays an important role in realizing a high-speed relay. In this paper, WT that represents a multi-level bandpass filter, is chosen. A suitable choice of a mother wavelet plays also a vital role in terms of speed and time-frequency localization. In this respect, the so-called "Piecewise Linear Spline Wavelet" is chosen since it is more suitable for transient signals analysis in terms of speed and time-frequency localization [15]. In this context, the high-pass filter of this wavelet has 3 coefficients, so it is simpler and speedier than other filters used in [6–12]. Fig. 4 shows the aforesaid mother wavelet with its transfer modulus.

The chosen wavelet is tuned to extract two signals of different bands of frequencies ( $I_H$ ,  $I_L$ ) from the fault induced HF transient current signal in a modal domain. The first signal,  $I_H$ , has frequencies band of [50–100 kHz], with center frequency of 75 kHz, which can be obtained by applying the DWT with detail 1 (d1), while the second signal,  $I_L$ , has frequencies band of [6.25–12.5 kHz], with center frequency of 9.37 kHz, which can be obtained by applying the

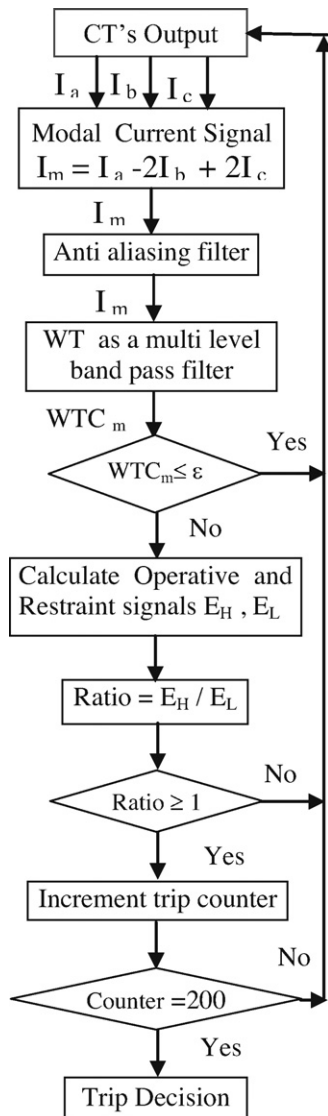


Fig. 3. A flowchart of the developed protection scheme.

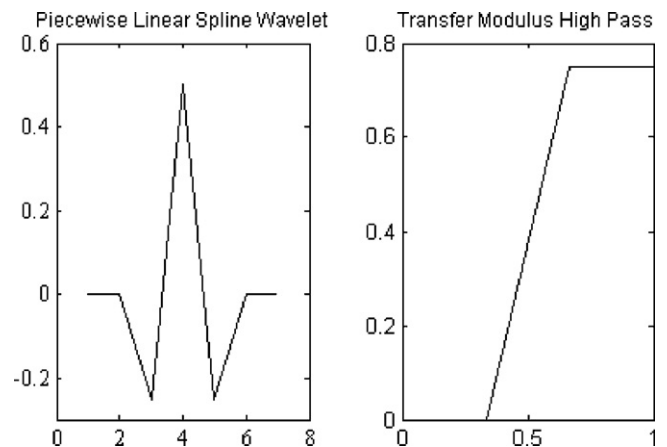


Fig. 4. A piecewise linear spline wavelet with its transfer modulus.

DWT with detail 4 (d4). However, in case of switching operation, HF transient signals are also induced, but their contents of frequencies are less than those induced by a fault as will be shown later in the simulation results. A threshold value ‘ $\varepsilon$ ’ is chosen to be compared with d1 coefficients to detect the abnormal condition, if a wavelet coefficient of d1 is more than this threshold the spectral energy routine will be triggered to compute the spectral energies ( $E_H, E_L$ ) of the captured signals ( $I_H, I_L$ ), respectively, over a 1.5 ms window length (300 samples), to produce the operative,  $E_{op}$ , and restraint,  $E_{re}$ , signals of the relay that are given as follows:

$$E_H(n) = E_{op}(n) = S \sum_{k=n-m}^n I_H^2(k) \quad (5)$$

$$E_L(n) = E_{re}(n) = \sum_{k=n-m}^n I_L^2(k) \quad (6)$$

where  $n$  represents the recent sample,  $m$  represents the number of samples in a chosen window and  $S$  represents a scaling factor, which is chosen to be 100 in this study.

The discriminating signals,  $E_{op}$  and  $E_{re}$ , are computed sample by sample and consequently the energy ratio is computed at each sample as follows:

$$\text{Ratio}(n) = \frac{E_{op}(n)}{E_{re}(n)} \quad (7)$$

If the energy ratio is  $\geq 1$  for 1 ms (200 sample), then the relay discriminates an internal fault and issues a trip signal, else the relay discriminates an external fault and restraint.

### 5. Protection scheme performance evaluation

In order to evaluate the performance of the developed protection scheme it is programmed in conjunction with WT using MATLAB environment. The EMTDC program [16] is used to simulate different types of faults at different positions, fault resistances and fault inception angles on a studied 400 kV–50 Hz power transmission system, shown in Fig. 2. The transmission line is ideally transposed and has a flat configuration with 10 m spacing between adjacent conductors and a ground resistivity of 100  $\Omega\text{m}$ . The used transmission line model is frequency dependent, the arc resistance is included in the fault model, and the busbar capacitance is included in the network model. The impedances values of the equivalent sources S1, S2, S3, and S4 in ohm are:  $Z_{s1} = 25$ ,  $Z_{s2} = 25$ ,  $Z_{s3} = 20$ ,  $Z_{s4} = 15$ , respectively. Two loads of (300 + j190) MVA/phase are placed at the each end of the line  $L_2$  to investigate the effect of heavy load switching on the performance of the introduced scheme. All fault currents are considered to be seen by the relay  $R_{yz}$ . A sampling frequency of 200 kHz is used in this study and a DWT with d1 and d4 is applied to extract the required bands of frequency from fault induced HF transient current signal in a modal domain.

Figs. 5–13 show the relay response curves for the studied cases. There are four graphs for each studied case: the first two graphs represent the DWT outputs at d1 and d4, respectively. The third graph shows the discriminating energy signals; where the solid curve represents the operative signal and the dotted curve represents the restraint signal. The solid curve in the fourth graph represents the energy ratio and the strait dashed line represents a threshold value (unity) for discriminating between the internal and external faults.  $R_f$  represents the fault resistance and  $\varphi$  represents the fault inception angle.

Fig. 5 depicts an internal single phase to ground fault ‘a–g’ at 50 km from bus ‘Y’ at line  $L_2$ . The energy ratio indicates clearly that there is an internal fault. As a result, the relay issues a trip signal.

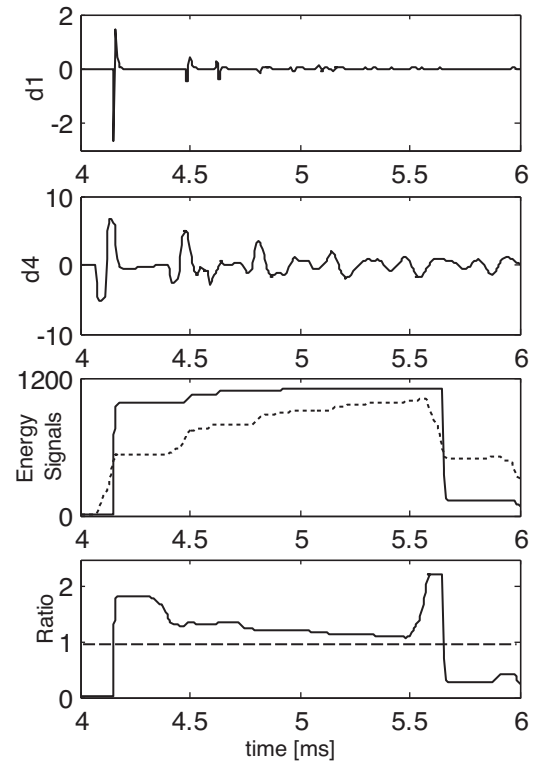


Fig. 5. ‘a–g’ fault on line  $L_2$  at 50 km from busbar ‘Y’,  $R_f = 0.5 \Omega$ ,  $\varphi = 90^\circ$ .

Fig. 6 depicts an external single phase to ground fault ‘a–g’ at line  $L_3$  at 70 km from busbar ‘Z’. It is obvious that the energy ratio is lower than unity; therefore, the relay indicates an external fault and restraints.

Fig. 7 depicts an external single phase to ground fault ‘a–g’ at line  $L_3$  at 200 m from busbar ‘Z’. Again, the energy ratio is lower than unity, therefore, the relay indicates an external fault and restraints.

Fig. 8 depicts the relay response to a single phase to ground fault ‘a–g’ at busbar ‘Z’. Since busbar ‘Z’ is out of the protection zone, then the energy ratio is lower than unity and the relay indicates an external fault and restraints.

Fig. 9, depicts the relay response to an internal single phase to ground fault ‘a–g’ at line  $L_2$  at 200 m from busbar ‘Z’. Since the energy ratio is more that unity the relay indicates an internal fault and issues a trip signal.

The results of the last three cases prove that the introduced scheme can discriminate between faults on and/or close to remote busbar (internal or external to the protected zone), in contrast to the protection scheme of [8].

Fig. 10 depicts the relay response to an internal high resistance fault ‘b–g’ ( $R_f = 300 \Omega$ ) at a mid point of line  $L_2$ . It is evident that the energy ratio is more than unity; therefore, the relay indicates an internal fault and issues a trip signal. Hence, the introduced relay is unaffected by the existence of high resistance in the fault path.

Fig. 11 depicts the relay response to an internal ‘b–g’ fault with phase inception angle  $\varphi = 0^\circ$  at a mid point of line  $L_2$ . As expected, the WT outputs are reduced in magnitude but their unique characteristics still exist, hence the energy ratio is more than unity. As a result, the relay indicates an internal fault and issues a trip signal. Hence, the introduced relay is unaffected by the fault inception angle.

Fig. 12 depicts the relay response to an external ‘a–b’ fault on line  $L_1$  at 200 m from busbar ‘Y’, with phase inception angle  $\varphi = 0^\circ$ . It is clear that the energy ratio is lower than unity; therefore, the relay indicates an external fault and restraints.

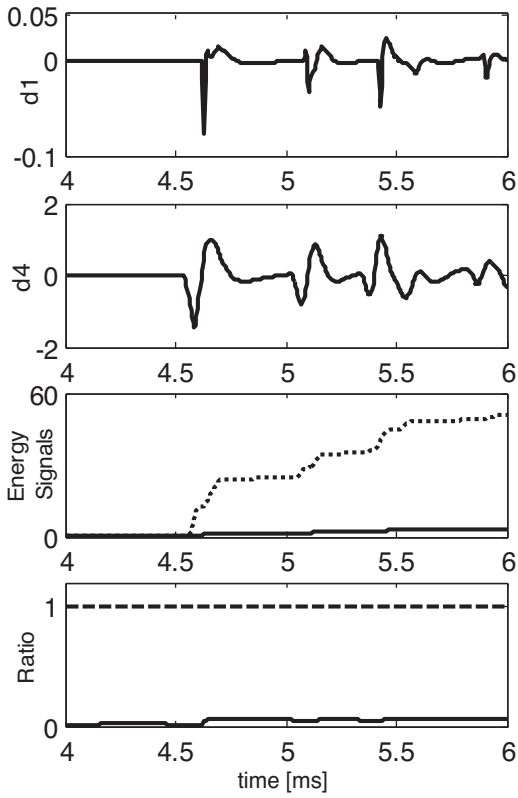


Fig. 6. 'a-g' fault on line  $L_3$  at 70 km from busbar 'Z',  $R_f = 0.5 \Omega$ ,  $\varphi = 90^\circ$ .

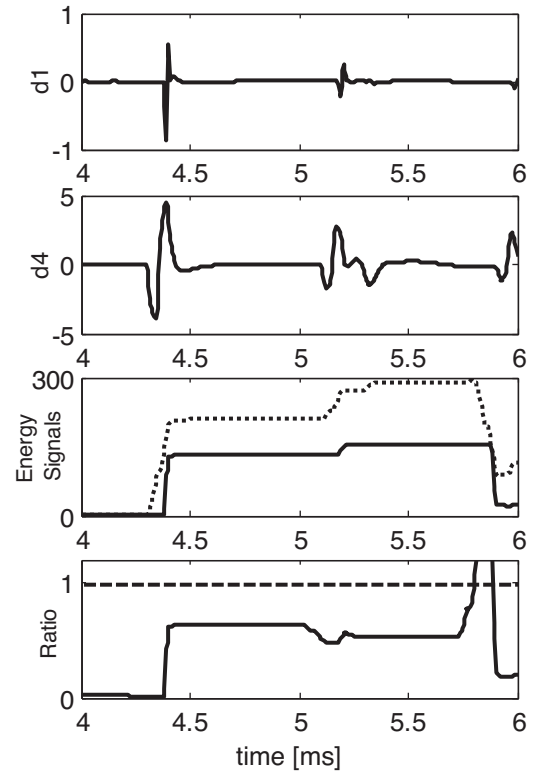


Fig. 8. 'a-g' fault on busbar 'Z',  $R_f = 0.5 \Omega$ ,  $\varphi = 90^\circ$ .

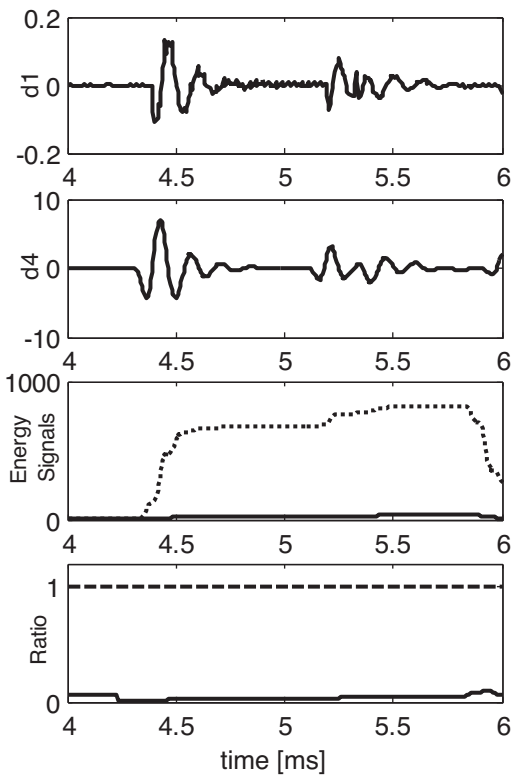


Fig. 7. 'a-g' fault on line  $L_3$  at 200 m from busbar 'Z',  $R_f = 0.5 \Omega$ ,  $\varphi = 90^\circ$ .

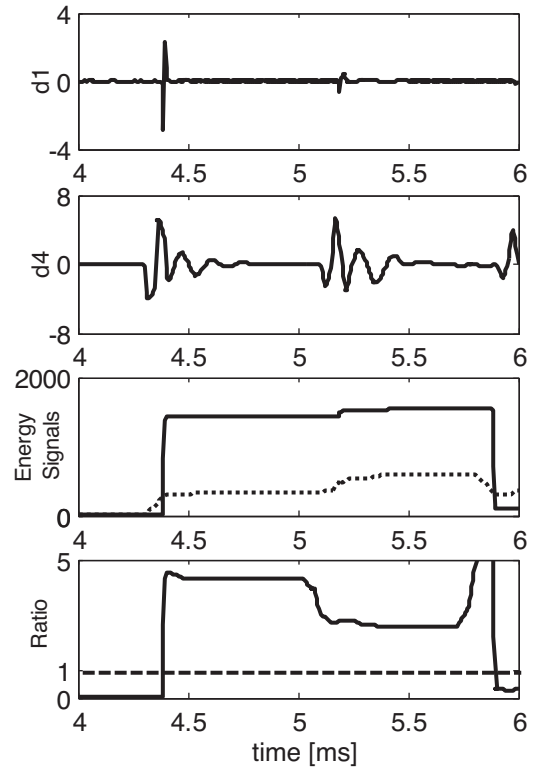


Fig. 9. 'a-g' fault on line  $L_2$  at 200 m from busbar 'Z',  $R_f = 0.5 \Omega$ ,  $\varphi = 90^\circ$ .

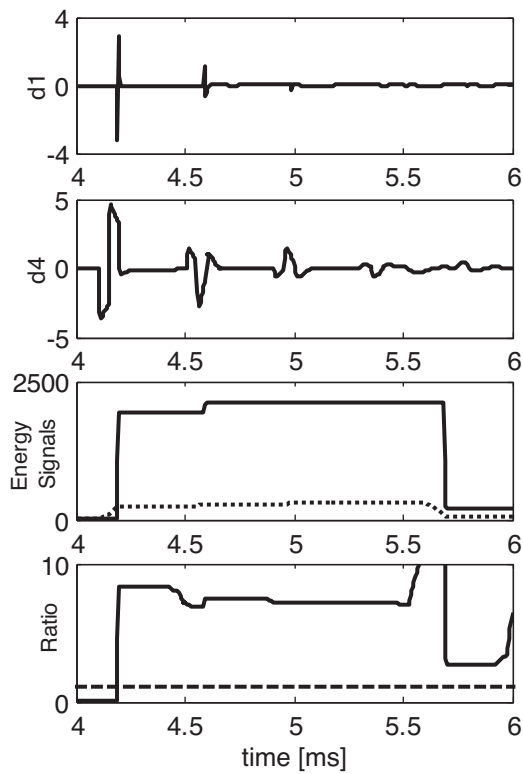


Fig. 10. 'b-g' fault at mid point of line  $L_2$ ,  $R_f = 300 \Omega$ ,  $\varphi = 90^\circ$ .

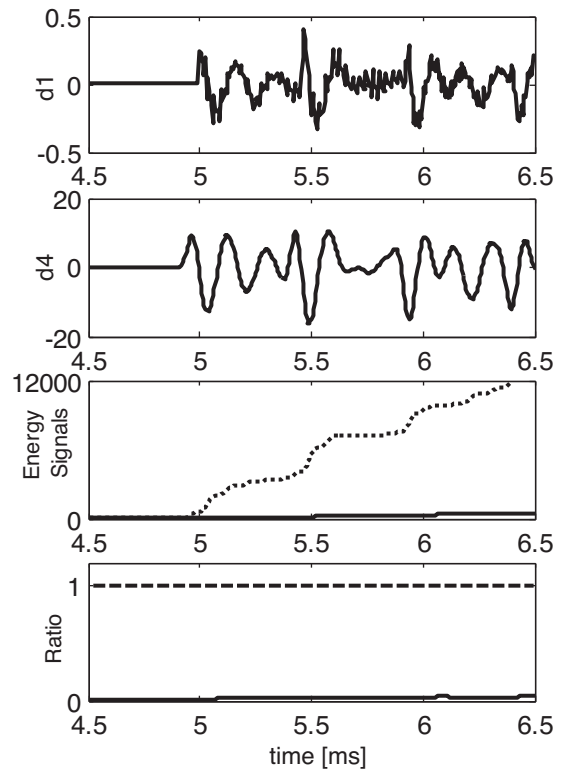


Fig. 12. 'a-b' fault on line  $L_1$  at 200 m from busbar 'Y',  $R_f = 0.5 \Omega$ ,  $\varphi = 0^\circ$ .

Fig. 13 depicts the relay response to an external 'a-b-c-g' fault at a mid point of line  $L_1$ . It is clear that the energy ratio is lower than unity; therefore, the relay indicates an external fault and restrains. Hence, one can conclude that the relay response is unaffected by the fault type.

The effect of non-fault transients on the protection scheme is tested for several cases, for example, Fig. 14, depicts the relay response to a heavy load switching at busbar 'Y'. It is clear that the energy ratio is lower than unity; hence, the relay can discriminate between faults and non-fault events successfully.

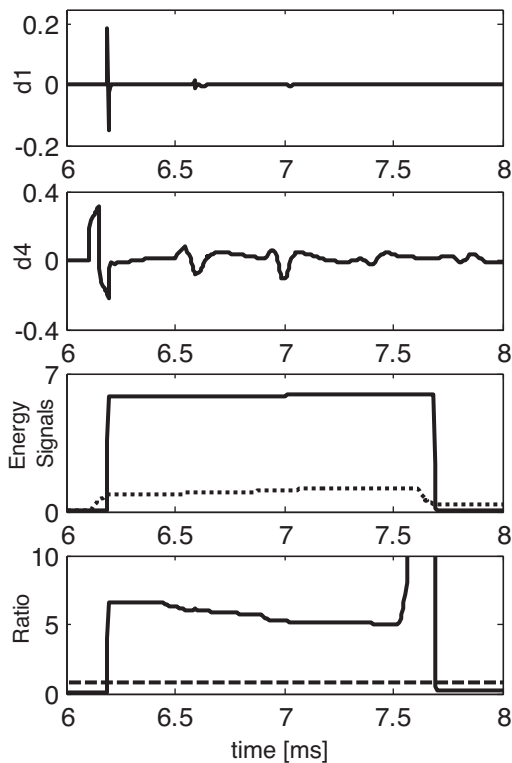


Fig. 11. 'b-g' fault at mid point of line  $L_2$ ,  $R_f = 0.5 \Omega$ ,  $\varphi = 0^\circ$ .

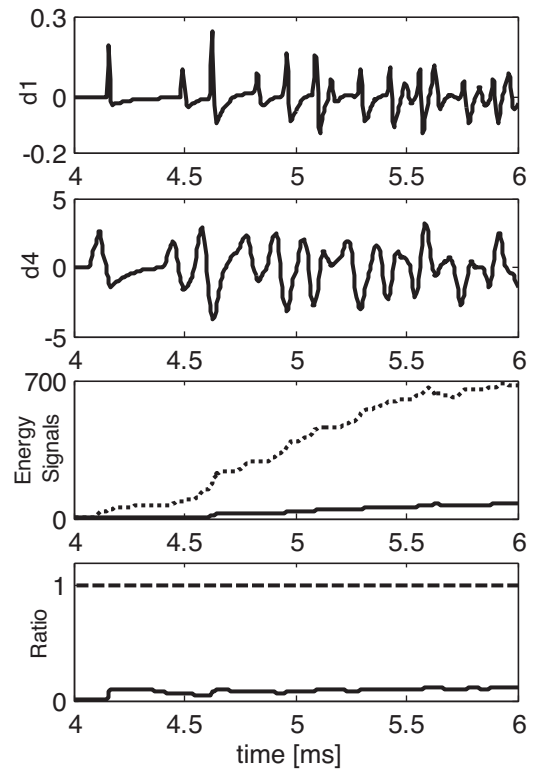


Fig. 13. 'a-b-c-g' fault at mid point of line  $L_1$ ,  $R_f = 0.5 \Omega$ ,  $\varphi = 90^\circ$ .

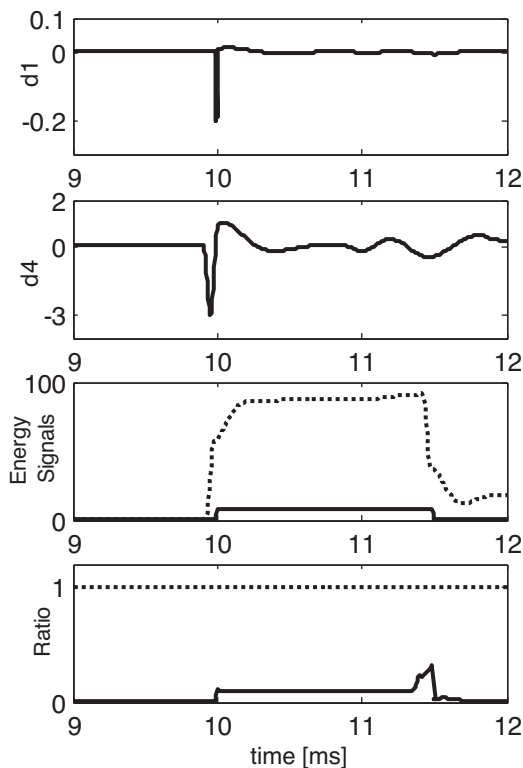


Fig. 14. Heavy load switching at busbar 'Y'.

## 6. Conclusion

This paper presented a high-speed noncommunication protection scheme based on WT, dedicated for entire transmission lines protection. The scheme has the communication protection discriminative properties without the need for communication channels linking the protection at each end of a line. It thus eliminates any loss of reliability, which might otherwise arise because of communication channels failure. The protection scheme utilizes a high-speed WT to extract two signals, each with distinct band of frequency, from the fault induced HF current signal in a modal domain. The spectral energies of the extracted signals are

then used as the discriminating signals of the relay (operative and restraint). Based on the ratio between these discriminating signals the relay can distinguish between the internal and external faults. The introduced scheme has the ability to discriminate the faulted line irrespective of the fault type, fault position, fault inception angle, and fault resistance. Moreover, it does not affected by any change in a system source parameters and system source configuration.

## References

- [1] W. Elmore, Protective Relaying Theory and Applications, second ed., Marcel Dekker, Inc., New York, 2005.
- [2] M. Chamia, S. Liberman, Ultra high speed relay for EHV/UHV transmission lines, *IEEE Transactions on Power Apparatus and Systems* 97 (1978) 2104–2112.
- [3] A.T. Johns, New ultra high speed directional comparison technique for the protection of EHV transmission lines, *IEE Proceeding on Generation Transmission and Distribution* 127(C) (1980) 228–239.
- [4] P.A. Crossley, P.G. McLaren, Distance protection based on traveling waves, *IEEE Transactions on Power Apparatus and Systems* 102 (9) (1983) 2971–2983.
- [5] L. Jie, S. Elangovan, B.X. Devotta, Adaptive traveling wave protection algorithm using two correlation functions, *IEEE Transactions on Power Delivery* 4 (1) (1999) 126–131.
- [6] A.T. Johns, R.K. Aggarwal, Z.Q. Bo, Non Unit protection technique for EHV transmission systems based on fault-generated noise part 1, signal measurement, *IEE Proceeding on Generation Transmission and Distribution* 141 (2) (1994) 133–140.
- [7] A.T. Johns, R.K. Aggarwal, Z.Q. Bo, Non Unit protection technique for EHV transmission systems based on fault-generated noise, part 2, signal processing, *IEE Proceeding on Generation Transmission and Distribution* 141 (2) (1994) 141–147.
- [8] Z.Q. Bo, A new noncommunication protection technique for transmission lines, *IEEE Transactions on Power Delivery* 13 (4) (1998) 1073–1078.
- [9] X.N. Lin, Z.Q. Bo, B.R. Caunce, Boundary protection using complex wavelet transform, in: *International APSCOM Conference, Hung Kong, 2003*, pp. 744–749.
- [10] O. Chaari, M. Meunier, Wavelets: a new tool for resonant grounded power distribution systems relaying, *IEEE Transactions on Power Delivery* 11 (3) (1996) 1301–1308.
- [11] A.I. Megahed, A.E. Bayoumy, Usage wavelet transform in the protection of series-compensated transmission lines, *IEEE Transactions on Power Delivery* 21 (3) (2006) 1213–1221.
- [12] J.D. Duan, J. Kuang, L. An, Research of boundary protection unit based on phase information of the improved recursive wavelet transform for EHV transmission lines, in: *10th IET International Conference on DPSP, 2010*.
- [13] D.C. Robertson, Wavelets and electromagnetic power system transients, *IEEE Transactions on Power Delivery* 11 (2) (1996) 1050–1058.
- [14] O. Rioul, M. Vetterli, Wavelet and signal processing, *IEEE Signal Processing Magazine* 8 (4) (1991) 14–38.
- [15] S. Gilbert, N. Truong, *Wavelets and Filter Banks*, Wellesley-Cambridge Press, USA, 1996.
- [16] EMTDC 2008, Manitoba HVDC Research Center, Canada.